Observation of a New Oxygen-Isotope-Sensitive Raman Band for Oxyhemoproteins and Its Implications in Heme Pocket Structures

Shun Hirota,[†] Takashi Ogura,[†] Evan H. Appelman,[‡] Kyoko Shinzawa-Itoh,[§] Shinya Yoshikawa,[§] and Teizo Kitagawa*,[†]

Contribution from the Institute for Molecular Science, Okazaki National Research Institutes and Graduate University for Advanced Studies, Myodaiji, Okazaki 444, Japan, Chemistry Division, Argonne National Laboratory, Argonne, Illinois 60439, and Department of Life Science, Faculty of Science, Himeji Institute of Technology, 1479-1, Kanaji, Kamigoricho, Akogun, Hyogo 678-12, Japan

Received May 23, 1994[⊗]

Abstract: A new oxygen-isotope-sensitive Raman band was found for oxyhemoglobin (HbO_2) and oxycytochrome *c* oxidase ($CcO{\cdot}O_2$) in the frequency region lower than the Fe−O_2 stretching mode (ν_{Fe-O_2}). This band was located at 425 cm^{-1} for $Hb^{16}O_2$ and shifted to 405 cm^{-1} with $Hb^{18}O_2$ and to ~423 and ~407 cm^{-1} with $Hb^{16}O^{18}O$. The corresponding band appeared at 435 cm^{-1} for $CcO{\cdot}^{16}O_2$ and shifted to 415 cm^{-1} with $CcO{\cdot}^{18}O_2$. Accordingly, the band has been assigned to the Fe−O−O bending mode (δ_{FeOO}). However, the corresponding band could not be identified for oxymyoglobin (MbO_2). The Fe−O_2 stretching mode (ν_{Fe-O_2}) was observed at 568, 567, 544, and 544 cm^{-1} for $Hb^{16}O_2$, $Hb^{16}O^{18}O$, $Hb^{18}O^{16}O$, and $Hb^{18}O_2$, respectively, and the corresponding modes were observed at 571, 569, 547, and 545 cm^{-1} for MbO_2 and 571, 567, 548, and 544 cm^{-1} for $CcO{\cdot}O_2$. The ν_{Fe-O_2} bandwidths of HbO_2 and MbO_2 were alike and 1.5 times broader than that of $CcO{\cdot}O_2$, suggesting that the Fe−O−O geometry is more nearly fixed in the latter. Despite the greatly different reactivities of bound O_2 in HbO_2 and $CcO{\cdot}O_2$, their ν_{Fe-O_2} and δ_{FeOO} frequencies and O_2-isotopic frequency shifts were alike, indicating similar Fe−O−O binding geometries. Normal coordinate calculations for an isolated three-atom molecule could reproduce the observed isotopic frequency shifts with the 115° bond angle reported for MbO_2, but not with the 155° angle reported for HbO_2.

Introduction

Among various derivatives of heme proteins the dioxygen adducts are the most important, since they are primarily involved in the functions of the proteins. These adducts have, indeed, been investigated extensively. Since the Fe−O_2 stretching frequency (ν_{Fe-O_2}) of the dioxygen adduct of heme proteins reflects the strength of the Fe−O_2 bond and thus the state of the bound O_2, the ν_{Fe-O_2} resonance Raman (RR) band has attracted attention in studies of model compounds as well as heme proteins.[1] The ν_{Fe-O_2} RR band has been identified for dioxygen adducts of hemoglobin (HbO_2),[2-4] myoglobin (MbO_2),[5] cytochrome P-450 ($P\text{-}450{\cdot}O_2$),[6-8] peroxidases,[9,10] and cytochrome *c* oxidase ($CcO{\cdot}O_2$).[11-13] The O−O stretching mode (ν_{OO}) was observed with IR spectroscopy for HbO_2 and MbO_2, and the presence of multiple species was noted.[14] However, none of these studies succeeded in observing the Fe−O−O bending mode (δ_{FeOO}), although for compound III of lactoperoxidase only another oxygen-isotope-sensitive Raman band was found at 491 cm^{-1} and assigned to the Fe−O−O bending mode.[10]

The Fe−O−O geometry of oxyhemoproteins, which should sensitively affect the δ_{FeOO} frequency, has not been established unambiguously by X-ray crystallographic analyses: the Fe−O−O angle is reported to be 115° for spermwhale Mb,[15a,b] 153 and 159° respectively for the α and β subunits of human Hb A,[16a,b] and 160° for the α subunit of an intermediately ligated $\alpha_{oxy}\beta_{deoxy}$ Hb.[17] X-ray-absorption near-edge structure (XANES)

[†] Okazaki National Research Institutes and Graduate University for Advanced Studies.
[‡] Argonne National Laboratory.
[§] Himeji Institute of Technology.
[⊗] Abstract published in *Advance ACS Abstracts*, October 15, 1994.

(1) Yu, N.-T.; Kerr, E. A. In *Biological Applications of Raman Spectroscopy*; Spiro, T. G., Ed.; Wiley-Interscience: New York, 1988; Vol. 3, pp 39-95.
(2) Brunner, H. *Naturwissenschaften* **1974**, *61*, 129.
(3) Nagai, K.; Kitagawa, T.; Morimoto, H. *J. Mol. Biol.* **1980**, *136*, 271-289.
(4) Duff, L. L.; Appelman, E. H.; Shriver, D. F.; Klotz, I. M. *Biochem. Biophys. Res. Commun.* **1979**, *90*, 1098-1103.
(5) Kerr, E. A.; Yu, N.-T.; Bartnicki, D. E.; Mizukami, H. *J. Biol. Chem.* **1985**, *260*, 8360-8365.
(6) Bangcharoenpaurpong, O.; Rizos, A. K.; Champion, P. M.; Jollie, D.; Sligar, S. G. *J. Biol. Chem.* **1986**, *261*, 8089-8092.
(7) Egawa, T.; Ogura, T.; Makino, R.; Ishimura, Y.; Kitagawa, T. *J. Biol. Chem.* **1991**, *266*, 10246-10248.
(8) Hu, S.; Schneider, A. J.; Kincaid, J. R. *J. Am. Chem. Soc.* **1991**, *113*, 4815-4822.
(9) Van Wart, H. E.; Zimmer, J. *J. Biol. Chem.* **1985**, *260*, 8372-8377.
(10) Hu, S.; Kincaid, J. R. *J. Am. Chem. Soc.* **1991**, *113*, 7189-7194.
(11) (a) Ogura, T.; Takahashi, S.; Shinzawa-Itoh, K.; Yoshikawa, S.; Kitagawa, T. *J. Am. Chem. Soc.* **1990**, *112*, 5630-5631. (b) Ogura, T.; Takahashi, S.; Shinzawa-Itoh, K.; Yoshikawa, S.; Kitagawa, T. *Bull. Chem. Soc. Jpn.* **1991**, *64*, 2901-2907. (c) Ogura, T.; Takahashi, S.; Hirota, S.; Shinzawa-Itoh, K.; Yoshikawa, S.; Appelman, E. H.; Kitagawa, T. *J. Am. Chem. Soc.* **1993**, *115*, 8527-8536.
(12) Han, S.; Ching, Y. C.; Rousseau, D. L. *Proc. Natl. Acad. Sci. U.S.A.* **1990**, *87*, 2491-2495.
(13) Varotsis, C.; Woodruff, W. H.; Babcock, G. T. *J. Am. Chem. Soc.* **1989**, *111*, 6439-6440.
(14) Potter, W. T.; Tucker, M. P.; Houtchens, R. A.; Caughey, W. S. *Biochemistry* **1987**, *26*, 4699-4707.
(15) (a) Phillips, S. E. V. *Nature* **1978**, *273*, 247-248. (b) Phillips, S. E. V. *J. Mol. Biol.* **1980**, *142*, 531-554.
(16) (a) Shaanan, B. *Nature* **1982**, *296*, 683-684. (b) Shaanan, B. *J. Mol. Biol.* **1983**, *171*, 31-59.
(17) Brzozowski, A.; Derewenda, Z.; Dodson, E.; Dodson, G.; Grabowski, M.; Liddington, R.; Skarzynski, T.; Vallely, D. *Nature* **1984**, *307*, 74-76.

0002-7863/94/1516-10564$04.50/0

studies[18] indicate that the Fe−O−O angle is 115° for both HbO_2 and MbO_2. There might be structural differences between the crystalline state and solutions, as indicated by an RR study of metMb and deoxyMb,[19] while hydrogen-bonding interaction between the bound O_2 and a distal histidine is noted for crystalline MbO_2 in a neutron diffraction study[20] and for solution HbO_2 in an RR study.[21] We are curious to know whether the structure of the FeOO unit has some correlation with reactivities of bound oxygen in solution.

For model compounds, on the other hand, the complicated pattern of the ν_{OO} RR band and apparent splitting of the oxygen-isotope-sensitive bands seen in IR spectra of HbO_2 have been satisfactorily interpreted in terms of vibrational coupling of bound O_2 with a trans ligand without assuming the presence of multiple conformations.[22] The RR bands corresponding to ν_{Fe-O_2} and δ_{FeOO} were reported at 488 and 279 cm^{-1} for (Pc)-FeO_2 (Pc = phthalocyaninine),[23] at 508 and 349 cm^{-1} for (TPP)-FeO_2 (TPP = tetraphenylporphyrin),[24a] and at 516 and 343 cm^{-1} for (TMP)FeO_2 (TMP = tetramesitylporphyrin),[24a] although a single band was observed at 509 cm^{-1} for (OEP)FeO_2 (OEP = octaethylporphyrin)[24a,b] and at 568 cm^{-1} for (T_{piv}PP)FeO_2 [T_{piv}PP = *meso*-tetra(α,α,α,α-*o*-pivaloylamidophenyl)porphyrin].[25] These observations suggested that the oxygen-isotope-sensitive RR band of HbO_2 around 570 cm^{-1} arose from the ν_{Fe-O_2} mode,[23] although there was a suggestion[26] that the behavior of isotopic frequency shifts of this kind[4] could be an indication of the δ_{FeOO} mode instead of ν_{Fe-O_2}. The presence of direct correlation between the ν_{Fe-O_2} frequencies and the Fe−trans ligand bond strength has been noted[27] and, moreover, an inverse linear correlation between the ν_{OO} and ν_{Fe-O_2} frequencies has been found, similar to the case of CO adducts of heme proteins.[28]

The RR studies of model compounds suggest possible identification of the δ_{FeOO} RR band for heme proteins. The location of the δ_{FeOO} frequency is quite important in molecular dynamics studies on O_2 adducts of heme proteins, since the Fe−O−O bending force constant, which mainly determines the energy necessary for distortion of the Fe−O−O geometry, should depend upon the δ_{FeOO} frequency. Accordingly, in this study, we have investigated RR spectra of two kinds of oxyhemoproteins, those with unreactive O_2 and those with O_2 to be activated. For the former category we looked at the $^{16}O^{18}O$ as well as $^{16}O_2$ and $^{18}O_2$ adducts of Mb and Hb, and for the latter we examined the same dioxygen adducts of CcO, which is the terminal enzyme of the respiratory chain and catalyzes reduction of O_2 to H_2O.

Experimental Procedures

Raman scattering was excited at 423.0 and 427.0 nm by the second harmonic of the output of a Ti−sapphire laser (Spectra Physics, Model 3900) pumped by an Ar^+ ion laser (Spectra Physics, Model 2045). The second harmonic was generated with a $KNbO_3$ crystal (VIGRO OPTICS, USA).[29] The detector was a cooled (−20 °C) diode array (PAR 1421HQ) attached to a single monochromator (Ritsu Oyo Kogaku DG-1000). Two interchangeable blazed-holographic gratings (500-nm blaze, 1200 grooves/mm; or 900-nm blaze, 1200 grooves/mm) were mounted to the monochromator. The former and latter were used in the first and second order, respectively, and therefore the latter has provided a higher resolution (~0.4 cm^{-1}/channel) than the former (~1.0 cm^{-1}/channel). The slit width and slit height used were 200 μm and 10 mm, respectively. The exciting laser beam was focused to ~50 μm and its power at the sample point was 4−10 mW. Measurements for MbO_2 and HbO_2 were carried out at room temperature with a spinning cell (3500 rpm) to avoid photodissociation of oxygen. Measurements for CcO·O_2 were carried out with the artificial cardiovascular system for pursuing enzymatic reactions[30] as described elsewhere.[11c] Raman shifts were calibrated with CCl_4 and acetone, and the uncertainties of peak positions were ±1 cm^{-1}.

Horse Mb (Sigma, type M630) was dissolved in 50 mM Tris−HCl buffer, pH 8.5, and subjected to gel filtration through Sephadex G-25 under O_2 after reduction by sodium dithionite. The MbO_2 thus obtained was diluted to 90 μM with 50 mM Tris−HCl buffer, pH 8.5. Human adult Hb was prepared according to the method of Geraci et al.,[31] and its concentration was adjusted to 50 μM (heme) with 50 mM Tris−HCl buffer, pH 8.5. Purification of bovine CcO and preparation of its O_2 adduct were described elsewhere.[32,11c] $^{16}O^{18}O$ was obtained by the Ce^{IV} oxidation of $H^{16}O^{18}OH$, which was synthesized by reacting $H^{18}OF$ with $H_2{}^{16}O$.[33] The earlier procedure was improved by fluorinating $H^{18}OH$ in acetonitrile to obtain a solution of $H^{18}OF$ stabilized as a complex with CH_3CN.[34,35] The mass analysis of $^{16}O^{18}O$ gave $^{16}O^{18}O/^{16}O^{16}O/^{16}O^{17}O/^{17}O^{18}O/^{18}O^{18}O$ = 94:2.2:2.2:0.1:1.4. The O_2-isotope adducts of Mb and Hb were obtained from their $^{16}O_2$ adducts by exposure of the sample to N_2 gas flow for more than 5 min followed by substitution of $^{18}O_2$ (98.2 atom %, ISOTEC Inc.) or $^{16}O^{18}O$ for N_2. The transient CcO·O_2, with a lifetime of 100 μs, was obtained by photolysis of CcO·CO, followed by oxygenation; the details of the experimental procedures have been described elsewhere.[11c]

Results

Figure 1 shows the RR spectra in the 600−200 cm^{-1} region for the $^{16}O_2$ (A), $^{16}O^{18}O$ (B), and $^{18}O_2$ (C) adducts of Hb A obtained with the higher resolution grating and the difference spectrum (D) between the $^{16}O_2$ and $^{18}O_2$ adducts. The Raman band of $Hb^{16}O_2$ at 568 cm^{-1} is shifted to 544 cm^{-1}, with $Hb^{18}O_2$. Although there are porphyrin bands at 586 and 544 cm^{-1}, and the isotopic frequency shifts are not self-evident, the difference spectrum gave a clear symmetric differential pattern, and accordingly the O_2-isotopic frequency shift is proven, in agreement with the previous assignments.[2,3] In addition to this, we note that there is another difference pattern with a peak at 425 cm^{-1} and a trough at 405 cm^{-1}. This feature is seen in the raw spectra, in which the relative intensities of the peaks at 423 and 407 cm^{-1} are altered between spectra A and C. The Raman spectrum of $Hb^{16}O^{18}O$ exhibits a pattern intermediate

(18) Congiu-Castellano, A.; Bianconi, A.; Dell'Ariccia, M.; Longa, S. D.; Giovannelli, A.; Burattini, E.; Castagnola, M. *Biochem. Biophys. Res. Commun.* **1987**, *147*, 31−38.
(19) Zhu, L.; Sage, J. T.; Champion, P. M. *Biochemistry* **1993**, *32*, 11181−11185.
(20) Phillips, S. E. V.; Schoenborn, B. P. *Nature* **1981**, *292*, 81−82.
(21) Kitagawa, T.; Ondrias, M. R.; Rousseau, D. L.; Ikeda-Saito, M.; Yonetani, T. *Nature* **1982**, *298*, 869−871.
(22) Proniewicz, L. M.; Bruha, A.; Nakamoto, K.; Kyuno, E.; Kincaid, J. R. *J. Am. Chem. Soc.* **1989**, *111*, 7050−7056.
(23) Bajdor, K.; Oshio, H.; Nakamoto, K. *J. Am. Chem. Soc.* **1984**, *106*, 7273−7274.
(24) (a) Proniewicz, L. M.; Paeng, I. R.; Nakamoto, K. *J. Am. Chem. Soc.* **1991**, *113*, 3294−3303. (b) Wagner, W. D.; Paeng, I. R.; Nakamoto, K. *J. Am. Chem. Soc.* **1988**, *110*, 5565−5567.
(25) Burke, J. M.; Kincaid, J. R.; Peters, S.; Gagne, R. R.; Collman, J. P.; Spiro, T. G. *J. Am. Chem. Soc.* **1978**, *100*, 6083−6088.
(26) Benko, B.; Yu, N.-T. *Proc. Natl. Acad. Sci. U.S.A.* **1983**, *80*, 7042−7046.
(27) Walters, M. A.; Spiro, T. G. *J. Am. Chem. Soc.* **1980**, *102*, 6857−6858.
(28) Oertling, W. A.; Kean, R. T.; Wever, R.; Babcock, G. T. *Inorg. Chem.* **1990**, *29*, 2633−2645.
(29) Ogura, T.; Kitagawa, T. To be submitted for publication.
(30) Ogura, T.; Yoshikawa, S.; Kitagawa, T. *Biochemistry* **1989**, *28*, 8022−8027.
(31) Geraci, G.; Parkhurst, L. J.; Gibson, Q. H. *J. Biol. Chem.* **1969**, *244*, 4664−4667.
(32) Yoshikawa, S.; Choc, M. G.; O'Toole, M. C.; Caughey, W. S. *J. Biol. Chem.* **1977**, *252*, 5498−5508.
(33) Appelman, E. H.; Thompson, R. C.; Engelkemeir, A. G. *Inorg. Chem.* **1979**, *18*, 909−911.
(34) Rozen, S.; Brand, M. *Angew. Chem., Int. Ed. Engl.* **1986**, *25*, 554−555.
(35) Appelman, E. H.; Dunkelberg, O.; Kol. M. *J. Fluorine Chem.* **1992**, *56*, 199−213.

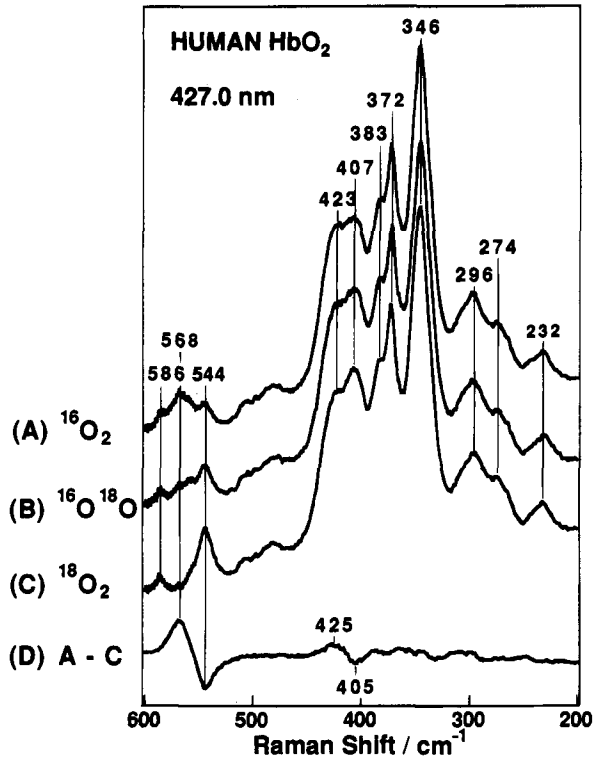

Figure 1. The RR spectra in the 600−200 cm^{-1} region of the $^{16}O_2$ (A), $^{16}O^{18}O$ (B), and $^{18}O_2$ adducts (C) of human Hb and the difference spectrum (D) between spectra A and C. The ordinate scales of spectra A−C are normalized by the intensity of the porphyrin bands. Experimental conditions: excitation—427.0 nm, 10 mW at the sample; grating of the monochromator—900-nm blaze, 1200 grooves/mm, second order; sample—50 μM (heme) in 50 mM Tris−HCl buffer, pH 8.5.

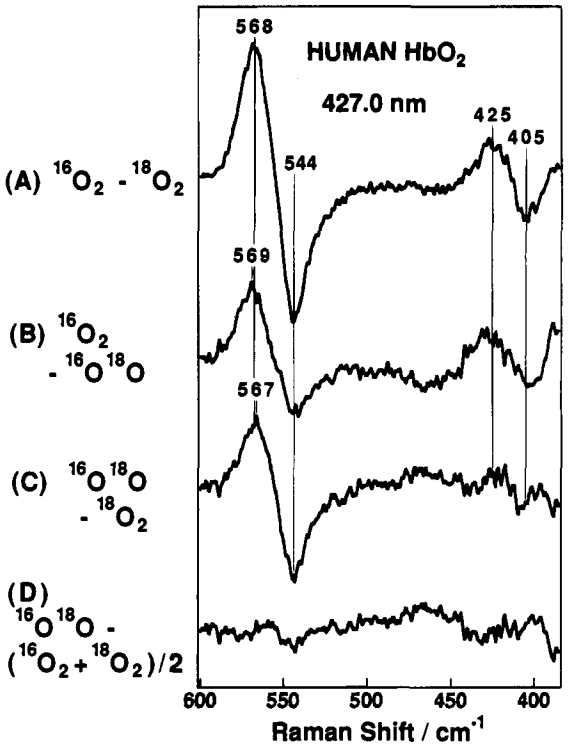

Figure 2. Differences between the spectra shown in Figure 1: (A) $Hb^{16}O_2 - Hb^{18}O_2$, (B) $Hb^{16}O_2 - Hb^{16}O^{18}O$, (C) $Hb^{16}O^{18}O - Hb^{18}O_2$, (D) $Hb^{16}O^{18}O - (Hb^{16}O_2 + Hb^{18}O_2)/2$. The ordinate scales of spectra A through D are the same.

between those of $Hb^{16}O_2$ and $Hb^{18}O_2$. In order to characterize the spectrum of $Hb^{16}O^{18}O$ more definitely, the difference spectra between the various spectra shown in Figure 1 were calculated and are displayed in Figure 2.

Spectrum A in Figure 2 is an expansion of spectrum D in Figure 1, making the difference peaks around 400 cm^{-1} more pronounced. While the ordinate scales in spectra B and C of Figure 2 are the same as that of spectrum A, the intensities of the positive peaks near 568 cm^{-1} and the negative peaks at 544 cm^{-1} are about one-half of those of spectrum A. This means that half the population of $Hb^{16}O^{18}O$ has the RR spectrum very close to that of $Hb^{16}O_2$, but the other half has that of $Hb^{18}O_2$. In other words, the ν_{Fe-O_2} frequency depends primarily on the mass of the oxygen atom directly bound to the Fe ion. However, we note that the position of the positive peak differs slightly among the three spectra: 568 cm^{-1} for A, 569 cm^{-1} for B, and 567 cm^{-1} for C. Such variation is not observed for the negative peaks. Spectrum D, representing spectrum B − (spectrum A + spectrum C)/2 of Figure 1, exhibits almost no difference pattern around 570 cm^{-1}, indicating that the $Fe^{16}O^{18}O$ stretching frequency is very close to that of $Fe^{16}O^{16}O$ and that the $Fe^{18}O^{16}O$ stretching frequency is close to that of $Fe^{18}O^{18}O$, in agreement with the previous observation by Duff et al.[4] This fact demonstrates the end-on binding of O_2 to the heme iron in the solution, although the same feature was previously noted as an indication of the δ_{FeOO} mode.[26] The difference pattern around 430−400 cm^{-1} is also seen in spectra B and C, but it is weaker than in spectrum A.

Figure 3 shows the RR spectra in the 600−300 cm^{-1} region of the $^{16}O_2$ (A), $^{16}O^{18}O$ (B), and $^{18}O_2$ (C) adducts of Mb and

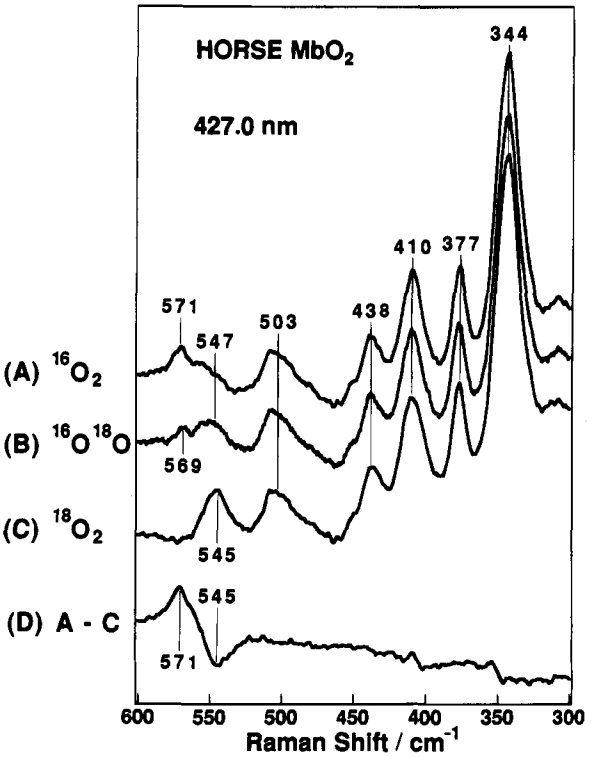

Figure 3. The RR spectra in the 600−300 cm^{-1} region of the $^{16}O_2$ (A), $^{16}O^{18}O$ (B), and $^{18}O_2$ adducts (C) of horse Mb and the difference spectrum (D) between spectra A and C. The ordinate scales of spectra A through C are normalized by the intensity of the porphyrin bands. Experimental conditions: excitation—427.0 nm, 5 mW at the sample; grating of the monochromator—500-nm blaze, 1200 grooves/mm, first order; sample—90 μM in 50 mM Tris−HCl buffer, pH 8.5.

the difference spectrum (D) between spectra A and C. To get more Raman intensity, the lower resolution grating was used

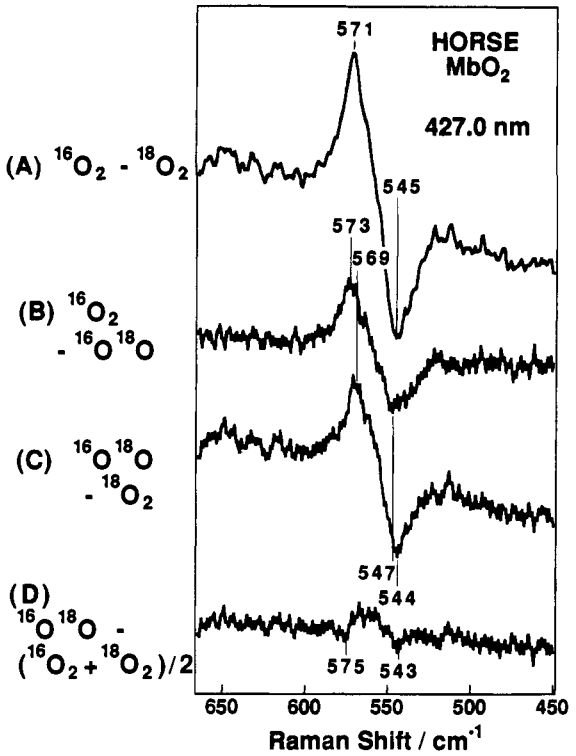

Figure 4. Differences of the RR spectra shown in Figure 3: (A) $Mb^{16}O_2 - Mb^{18}O_2$, (B) $Mb^{16}O_2 - Mb^{16}O^{18}O$, (C) $Mb^{16}O^{18}O - Mb^{18}O_2$, (D) $Mb^{16}O^{18}O - (Mb^{16}O_2 + Mb^{18}O_2)/2$. The ordinate scales of spectra A–D are the same.

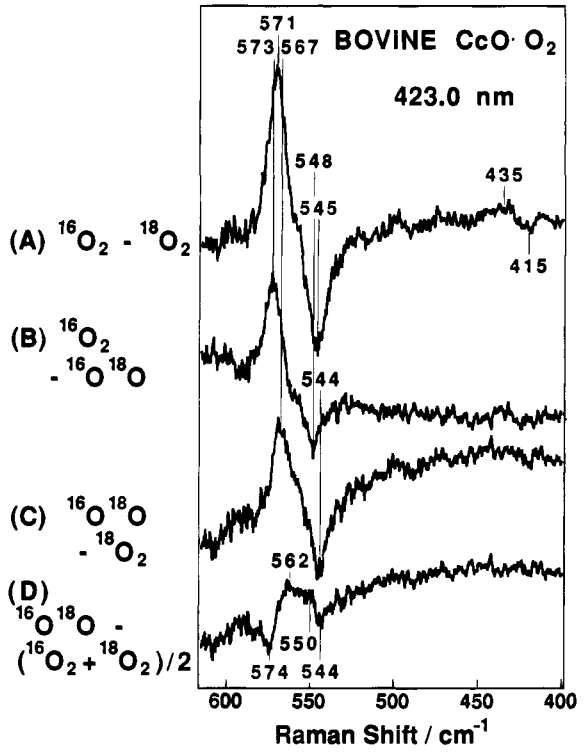

Figure 5. Differences of the RR spectra of O_2-isotope adducts of CcO: (A) $CcO{\cdot}^{16}O_2 - CcO{\cdot}^{18}O_2$, (B) $CcO{\cdot}^{16}O_2 - CcO{\cdot}^{16}O^{18}O$, (C) $CcO^{16}O^{18}O - CcO{\cdot}^{18}O_2$, (D) $CcO{\cdot}^{16}O^{18}O - (CcO^{16}O_2 + CcO{\cdot}^{18}O_2)/2$. Ordinate scales of spectra A through D are the same. Experimental conditions: pump beam—590 nm, 210 mW at the sample; probe beam—423.0 nm, 4 mW at the sample; grating of the monochromator—500-nm blaze, 1200 grooves/mm, first order; delay time after CO photodissociation in the O_2 atmosphere—100 μs.

in these measurements. The RR spectrum of MbO_2 in this frequency region is distinct from that of HbO_2 shown in Figure 1, although the RR spectra of the two species are alike in the frequency region higher than 1200 cm^{-1}. In particular, the 503 cm^{-1} band of MbO_2 is absent for HbO_2, and the 438 cm^{-1} band of MbO_2 is shifted to 423 cm^{-1} for HbO_2. The latter suggests that geometrical structures of the vinyl side chains of the porphyrin are appreciably different between the two proteins.

The RR band of spectrum A at 571 cm^{-1} is shifted to 545 cm^{-1} in spectrum C. Although the 545 cm^{-1} band appears more intense than the one at 571 cm^{-1}, spectrum D displays a symmetric differential pattern, indicating that the 571 cm^{-1} band of MbO_2 undergoes a shift by 26 cm^{-1} upon $^{18}O_2$ substitution similar to the shift of the 568 cm^{-1} band of HbO_2. The 571 cm^{-1} band is thus assignable to the ν_{Fe-O_2} mode. In contrast with the results for HbO_2, there is no trace of a differential pattern in the lower frequency region. Since the ν_{Fe-O_2} band in the RR spectrum of $Mb^{16}O^{18}O$ is obscured due to the presence of porphyrin bands in the same frequency region, difference spectra were calculated in the same way as for HbO_2.

Spectrum A in Figure 4 is the same as spectrum D in Figure 3. While the ordinate scales in spectra B–D are the same as that of spectrum A, the peaks in spectra B and C are significantly weaker than those in spectrum A. The position of the positive peak shifts from 571 to 573 to 569 cm^{-1} in spectra A–C, while that of the negative peak shifts from 545 to 547 to 544 cm^{-1}, suggesting that the peak frequencies of the ν_{Fe-O_2} bands of $Mb^{16}O^{18}O$ and $Mb^{18}O^{16}O$ are slightly different from those of $Mb^{16}O_2$ and $Mb^{18}O_2$, respectively. In fact, spectrum D, which represents spectrum B − (spectrum A + spectrum C)/2 of Figure 3, displays a small double-well pattern.

Figure 5 shows the same set of difference spectra observed for $CcO{\cdot}O_2$ excited at 423 nm. The $^{16}O_2/^{18}O_2$ difference spectrum (A) gives a positive peak at 571 cm^{-1} and a negative peak at 545 cm^{-1}, similar to the spectrum of $Mb^{16}O_2/Mb^{18}O_2$. In spectra B and C the positive peak shifts to 573 and 567 cm^{-1}, respectively, while the negative peak shifts to 548 and 544 cm^{-1}, respectively. The shifts are slightly larger than those of MbO_2. We stress that spectrum A displays a difference pattern at 435/415 cm^{-1} similar to that in Figure 2, although the corresponding peaks are extremely weak in spectra B and C. Difference spectrum D, representing a difference of the type $CcO{\cdot}^{16}O^{18}O - (CcO{\cdot}^{16}O_2 + CcO{\cdot}^{18}O_2)/2$, shows a definite double-well pattern, demonstrating that the O_2 binding is of an end-on type.[11c]

Discussion

The Fe−O_2 Stretching Mode. Analysis of the ν_{Fe-O_2} RR band of heme proteins has been obscured due to the presence of nearby porphyrin bands. In fact, the raw spectra shown in Figures 1 and 3 include a few side bands around 550 cm^{-1}. However, those side bands can be canceled in the isotope-difference spectra, and thus the oxygen-associated RR bands can be extracted. In order to determine the ν_{Fe-O_2} frequency precisely, we carried out simulation calculations of the isotope difference spectra by assuming a Gaussian band shape with an appropriate peak intensity and bandwidth in common to the $Fe^{16}O^{16}O$, $Fe^{16}O^{18}O$, $Fe^{18}O^{16}O$, and $Fe^{18}O^{18}O$ adducts. The results are illustrated in Figure 6, where (A), (B), (C), and (D) represent the assumed bands, the experimental difference spectra, the calculated difference spectra, and residuals between the experimental and calculated difference spectra, respectively, in common to the difference combinations of (a) $Mb^{16}O_2$ −

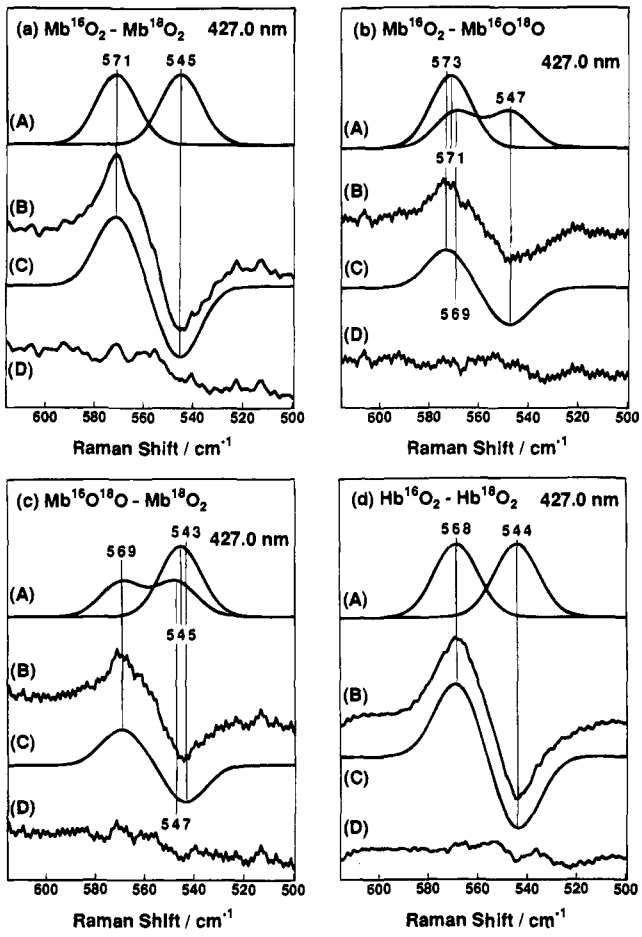

Figure 6. Simulation of the difference spectra of MbO_2 and HbO_2: (A) assumed bands (Gaussian band shape, bandwidth is 20 cm^{-1} for MbO_2 and 21 cm^{-1} for HbO_2), (B) experimental difference spectra, (C) calculated difference spectra, and (D) residuals between the experimental and calculated difference spectra.

$Mb^{18}O_2$, (b) $Mb^{16}O_2 - Mb^{16}O^{18}O$, (c) $Mb^{16}O^{18}O - Mb^{18}O_2$, and (d) $Hb^{16}O_2 - Hb^{18}O_2$. In all four panels, the residuals are reduced to the noise level of the spectra, and therefore the spectral parameters used, including band positions and bandwidths, are considered to characterize the observed bands correctly. For $Hb^{16}O^{18}O$ the two peak positions are so close to those of $Hb^{16}O_2$ and $Hb^{18}O_2$ that the other combinations are similar to $Hb^{16}O_2 - Hb^{18}O_2$.

The bandwidths thus obtained are 20 cm^{-1} for MbO_2, 21 cm^{-1} for HbO_2, and 12.9 cm^{-1} for $CcO{\cdot}O_2$. We stress that the ν_{Fe-O_2} bandwidths of MbO_2 and HbO_2 are alike, but distinctly greater than that of $CcO{\cdot}O_2$. This does not depend upon the resolution of the spectrometer, since the higher-resolution grating was used for HbO_2 and the lower-resolution one was used for MbO_2 and $CcO{\cdot}O_2$. One might think that the large bandwidth for HbO_2 is due to an appreciable difference in the ν_{Fe-O_2} frequencies of the α and β subunits, since according to the X-ray study[16b] the Fe–O_2 bond lengths are 1.66 Å for the α and 1.87 Å for the β subunits. However, this interpretation seems less likely since the bandwidth of HbO_2 is almost the same as that of MbO_2. If the ν_{Fe-O_2} band is relatively sharp and its frequency differs slightly between $Fe^{16}O^{16}O$ and $Fe^{16}O^{18}O$ and between $Fe^{18}O^{16}O$ and $Fe^{18}O^{18}O$, the difference spectrum of a $^{16}O^{18}O - (^{16}O_2 + {}^{18}O_2)/2$ type would give rise to two positive and two negative peaks (double-well type). When the band becomes broader at the same frequency separation or when the frequency separations between the $Fe^{16}O^{16}O$ and $Fe^{16}O^{18}O$ adducts and between the $Fe^{18}O^{16}O$ and $Fe^{18}O^{18}O$ adducts become smaller without change in width, the double-well character of the difference spectrum becomes obscure. In fact, this type of difference spectra is less distinct in Figures 2 and 4 than in Figure 5, presumably for these two reasons.

The smaller width of the ν_{Fe-O_2} band for $CcO{\cdot}O_2$ would suggest that O_2 in $CcO{\cdot}O_2$ has a more tightly fixed geometry at the binding site than do MbO_2 and HbO_2. However, it is rather unexpected that, except for this difference in mobility, the bound O_2 in $CcO{\cdot}O_2$ quite closely resembles that in HbO_2 and MbO_2, even though there are distinct differences in their reactivities.

The Fe–O–O Bending Mode. The present experiments reveal the presence of another oxygen-isotope-sensitive band around 400 cm^{-1} for HbO_2 and $CcO{\cdot}O_2$ besides the band around 570 cm^{-1}. Since the new isotope-sensitive band overlaps the $C_\beta C_a C_b$ bending mode[36,37] of the 2- and 4-vinyl groups at 407 and 423 cm^{-1}, it is hard to observe it in the raw spectrum. Clarification of its presence has required the measurement of two oxygen-isotope adducts under highly controlled conditions. The $^{16}O_2$–$^{18}O_2$ difference peaks were noticed for the first time at 425/405 cm^{-1} for HbO_2 and at 435/415 cm^{-1} for $CcO{\cdot}O_2$. These bands were not shifted to intermediate frequencies with $^{16}O^{18}O$, as shown in Figures 2 and 5. Despite great efforts, the corresponding band could not be recognized for MbO_2, even with the higher-resolution grating.

For compound III of lactoperoxidase two pairs of oxygen-isotope-sensitive Raman bands have been observed at 531/513 and 491/482 cm^{-1} for the $^{18}O_2/^{16}O_2$ derivatives.[10] The latter pair was discernible when compound III was obtained from the reaction of compound II with $H_2{}^{16}O_2$ or $H_2{}^{18}O_2$ but not when it was obtained from the reactions of reduced enzyme with $^{16}O_2$ or $^{18}O_2$ and of oxidized enzyme with $H_2{}^{16}O_2$ or $H_2{}^{18}O_2$, while the former pair was observed for all three reactions. The 531/513 cm^{-1} pair was assigned to the Fe–O_2 stretching vibration and its unusually low frequency was attributed to increased delocalization of electrons to O_2 which is presumed to interact with the distal arginine. The other pair at 491/482 cm^{-1} was assigned to the δ_{FeOO} mode. This was the first suggestion for the appearance of the δ_{FeOO} RR band of heme proteins,[10] although it has not been acknowledged widely, partially due to the fact that the corresponding band was not clearly recognized for the Fe–O_2 compound derived in a normal way, that is, a reaction of reduced enzyme with dioxygen.

For nitric oxide adducts of ferrous heme proteins, such as MbNO, HbNO, and P-450·NO, the Fe–NO stretching (ν_{Fe-NO}) and Fe–N–O bending (δ_{FeNO}) modes have been observed around 550 and 450 cm^{-1}, respectively. The ν_{Fe-NO} frequencies, which show a zigzag dependence on the increase of the total mass of NO,[38,39] are sensitive to the mass of the atom bound to the iron ion but rather insensitive to the mass of the second atom. The ν_{Fe-O_2} frequencies of the O_2 adducts exhibit the same character as ν_{Fe-NO} regarding sensitivity to the mass of the atom bound to Fe. The frequencies of the other oxygen-isotope-sensitive bands of HbO_2 and $CcO{\cdot}O_2$ are close to the δ_{FeNO} frequency. Accordingly, it seems reasonable to assign the new oxygen-isotope-sensitive bands found in this study to δ_{FeOO}. However, the δ_{FeOO} frequencies of the end-on type Fe–O_2 porphyrins are reported around 350 cm^{-1}, and their $^{18}O_2$ isotopic

(36) Lee, H.; Kitagawa, T.; Abe, M.; Pandey, R. K.; Leung, H.-K.; Smith, K. M. *J. Mol. Struct.* **1986**, *146*, 329–347.
(37) (a) Hu, S.; Morris, I. K.; Sinch, J. P.; Smith, K. M.; Spiro, T. G. *J. Am. Chem. Soc.* **1993**, *115*, 12446–12458. (b) Choi, S.; Spiro, T. G.; Langry, K. C.; Smith, K. M. *J. Am. Chem. Soc.* **1982**, *104*, 4337–4344.
(38) Tsubaki, M.; Yu, N.-T. *Biochemistry* **1982**, *21*, 1140–1144.
(39) Hu, S.; Kincaid, J. R. *J. Am. Chem. Soc.* **1991**, *113*, 9760–9766.

Table 1. Observed Frequencies of MbO_2 and HbO_2 and Calculated Frequencies of the Isolated FeOO Unit[a]

		$^{16}O_2$		$^{18}O^{16}O$		$^{16}O^{18}O$		$^{18}O_2$	
		obs	calc	obs	calc	obs	calc	obs	calc
Mb[b]	ν_{OO}	~1130[d]	1133		1102		1100		1068
	ν_{Fe-O_2}	571	570	547	547	569	568	545	546
	δ_{FeOO}	(425)[e]	424	(~423)	417	(~407)	410	(405)	404
Hb[c]	ν_{OO}	~1130[d]	1130		1095		1102		1065
	ν_{Fe-O_2}	568	568	544	556	567	557	544	546
	δ_{FeOO}	425	425	~407	410	~423	417	405	402

[a] In cm^{-1}. [b] Parameters used for calculations are the following: r(Fe−O) = 1.83 Å, r(O−O) = 1.4 Å, K_1(Fe−O) = 2.18 mdyn/Å, K_2(O−O) = 5.7 mdyn/Å, H(Fe−O−O) = 0.58 mdyn·Å, F(Fe···O) = 1.28 mdyn/Å, θ(Fe−O−O) = 115°. [c] Parameters used for calculations are the following: r(Fe−O) = 1.83 Å, r(O−O) = 1.4 Å, K_1(Fe−O) = 2.52 mdyn/Å, K_2(O−O) = 5.15 mdyn/Å, H(Fe−O−O) = 0.75 mdyn·Å, F(Fe···O) = 1.28 mdyn/Å, θ(Fe−O−O) = 155°. [d] The ν_{OO} frequencies are estimated on the basis of the observed frequencies reported by ref 14 and the vibronic coupling described by ref 22. [e] Frequencies observed for HbO_2.

frequency shifts are extremely small (~5 cm^{-1}), and furthermore, the δ_{FeOO} frequency of compound III of lactoperoxidase is reported at 491 cm^{-1} and its $^{18}O_2$ isotopic frequency shift is almost half of the present observation. In order to see how large the isotopic frequency shifts are expected to be for the δ_{FeOO} mode with end-on geometry, normal coordinate calculations were carried out for an isolated three-atom molecule of FeOO.

Normal Coordinate Calculations. In the same way as our previous treatments for the CO adducts,[40,41] the Urey−Bradley force field represented by eq 1 was assumed:

$$2V = K_1(\Delta r_{Fe-O_2})^2 + K_2(\Delta r_{OO})^2 + H(\Delta\theta_{FeOO})^2 + F(\Delta q_{Fe\cdots O})^2 \quad (1)$$

where Δr_{Fe-O_2}, Δr_{OO}, $\Delta\theta_{FeOO}$, and $\Delta q_{Fe\cdots O}$ denote the displacement coordinates for the Fe−O_2 bond length, O−O bond length, Fe−O−O bond angle, and Fe···O nonbonding-atoms separation, respectively. The calculated frequencies are compared with the observed frequencies in Table 1. The equilibrium bond lengths used for MbO_2 were those obtained from the X-ray crystallographic analyses:[15a,b] r_{Fe-O_2} = 1.83 Å, r_{O-O} = 1.4 Å, and θ_{FeOO} = 115°. The force constants used were K_1 = 2.18 mdyn/Å, K_2 = 5.7 mdyn/Å, H = 0.58 mdyn·Å, and F = 1.28 mdyn/Å. They were adjusted to reproduce the observed frequencies of MbO_2. The size of F determines the magnitude of vibrational coupling between the stretching and bending coordinates. F = 1.3 mdyn/Å seems to be slightly larger than expected, but if a smaller value were assumed for F, a larger K_1 would be needed to reproduce the observed ν_{Fe-O_2} frequency. However, this would yield O_2-isotopic frequency shifts that were too large. For HbO_2 the calculations could not reproduce the observed results satisfactorily, in particular for the ν_{Fe-O_2} frequency of the $^{16}O^{18}O$ adduct, so long as the bending angle was assumed to be 155°, which is intermediate between the angles reported for the α and β subunits of HbO_2.[16a,b] The best fitted data shown in Table 1 were obtained with K_1 = 2.52 mdyn/Å, K_2 = 5.15 mdyn/Å, and H = 0.75 mdyn·Å, but the fitting level regarding the O_2-isotopic frequency shifts was not always satisfactory and was not improved when F was changed from 1.3 to 0.3 mdyn/Å. Since the ν_{Fe-O_2} frequencies and their $^{16}O^{18}O$ isotopic frequency shifts for HbO_2 are very close to those for MbO_2, it is unreasonable to assume different Fe−O−O bend angles between HbO_2 and MbO_2. This may suggest that the Fe−O−O geometry of HbO_2 is altered upon crystallization, as pointed out in the XANES study.[18] Such a structural change upon crystallization is, in fact, reported for Mb, for which some perturbation takes place in the Fe−His bond of the deoxy state,[19] and for which relative populations of different conformers of the CO adducts[42] differ between the crystal and solution states.[43]

Differences in the Fe−O−O Binding Geometry among Heme Proteins. The difference spectra of a $^{16}O^{18}O$ − ($^{18}O_2$ + $^{16}O_2$)/2 type were appreciably different among MbO_2, HbO_2, and CcO·O_2 (Figures 2D, 4D, and 5D). The difference between MbO_2 and HbO_2 arises from differences in proximity of the Fe−$^{16}O^{18}O$ frequency to the Fe−$^{16}O^{16}O$ frequency and of the Fe−$^{18}O^{16}O$ frequency to the Fe−$^{18}O^{18}O$ frequency, since the widths of the ν_{Fe-O_2} bands of MbO_2 and HbO_2 are alike; the most plausible values for the difference between the Fe−$^{16}O^{18}O$ and Fe−$^{16}O^{16}O$ stretching frequencies are <1, 2, and 4 cm^{-1}, respectively, for HbO_2, MbO_2, and CcO·O_2. Accordingly, the Fe−O−O valence angle is considered to increase in this order. It is possible in principle to estimate the difference in angle on the basis of normal coordinate calculations for different geometries without changing the force constants, but we refrain from reporting the values, since the force field and the molecular model used are not sufficiently precise to warrant such a calculation. However, it is evident even from this level of calculation that the new Raman band observed around 425 cm^{-1} is reasonably explained in terms of the δ_{FeOO} mode, despite the fact that the $^{18}O_2$ isotopic shifts are significantly larger than those of the Fe−porphyrin dioxygen complexes.[24]

The large difference between the δ_{FeOO} frequencies of lactoperoxidase and Hb presumably arises from the strong interaction between the terminal oxygen and the distal arginine postulated for lactoperoxidase,[10] since such interaction generally increases the energy required for movements of atoms along the bending coordinate and thus raises the bending frequency. The difference of the $^{18}O_2$ isotopic frequency shifts indicates the difference in the atomic displacement of oxygen atoms during the vibration. Accordingly, the large difference in the $^{18}O_2$ isotopic frequency shifts between lactoperoxidase and Hb means appreciable difference in the Fe−O−O valence angle.

The δ_{FeOO} RR band was observable for HbO_2 but not for MbO_2. A similar difference between Hb and Mb is present in the RR spectra of their CO adducts. The assignment of the Fe−C−O bending RR band is currently under debate; the band has been located at a frequency (~570 cm^{-1}) higher than that of the Fe−CO stretching (ν_{Fe-CO}) mode,[44] but recently a new CO-isotope-sensitive band was found around 350 cm^{-1} for HbCO, CcO·CO, and P-450·CO and was assigned to the δ_{FeCO} fundamental.[41] The fact that the new δ_{FeCO} frequency is lower than the Fe−CO stretching frequency is compatible with the present observation that the δ_{FeOO} frequency is lower than the Fe−O_2 stretching frequency. We note that only for Mb among various heme proteins examined could the δ_{FeCO} fundamental not be observed. The absence of the bending RR band for the O_2 and CO adducts might be characteristic of Mb, although its reason cannot be explained at the present stage. This may suggest that there is a factor controlling the RR intensity of the

(40) Nagai, M.; Yoneyama, Y.; Kitagawa, T. *Biochemistry* **1991**, *30*, 6495−6503.
(41) Hirota, S.; Ogura, T.; Shinzawa-Itoh, K.; Yoshikawa, S.; Nagai, M.; Kitagawa, T. *J. Phys. Chem.* **1994**, *98*, 6652−6660.
(42) Mourant, J. R.; Braunstein, D. P.; Chu, K.; Frauenfelder, H.; Nienhaus, G. U.; Ormos, P.; Young, R. D. *Biophys. J.* **1993**, *65*, 1496−1507.
(43) Zhu, L.; Sage, J. T.; Rigos, A. A.; Morikis, D.; Champion, P. M. *J. Mol. Biol.* **1992**, *224*, 207−215.
(44) Ray, G. B.; Li, X. Y.; Ibers, J. A.; Sessler, J. L.; Spiro, T. G. *J. Am. Chem. Soc.* **1994**, *116*, 162−176.

bending mode in the protein structure of the heme pocket and that this part of structure is different between Mb and Hb.

Conclusions

We have identified the Fe−O−O bending Raman band for dioxygen complexes of hemoglobin and cytochrome *c* oxidase for the first time. The band was located at 425 cm^{-1} for $Hb^{16}O_2$, shifted to 405 cm^{-1} with $Hb^{18}O_2$, and at 435 cm^{-1} for $CcO{\cdot}^{16}O_2$, shifted to 415 cm^{-1} with $CcO{\cdot}^{18}O_2$. We failed to identify the corresponding band for MbO_2. The Fe−O_2 stretching Raman band has also been observed for $^{16}O_2$, $^{18}O_2$, and $^{16}O^{18}O$ adducts of Hb, Mb, and CcO. The isotopic frequency shifts suggested that the Fe−O−O angles of these proteins are closer to 115° than to 155°. The bandwidth of the ν_{Fe-O_2} RR band indicated that the dioxygen is more tightly fixed in $CcO{\cdot}O_2$ than in HbO_2 and MbO_2.

Acknowledgment. The authors thank Prof. M. Nagai of Kanazawa University for her courtesy of giving them purified human Hb A and Prof. J. Kincaid of Marquette University for communicating to us their results. Preparation of $^{16}O^{18}O$ was carried out at Argonne National Laboratory under the auspices of the office of Basic Energy Sciences, Division of Chemical Sciences, U.S. Department of Energy. This study was supported in part by Grant-in-Aid of the Ministry of Education, Science, and Culture Japan for Priority Areas (Bioinorganic Chemistry) to T.K. (No. 04225106) and (Cell Energetics) to T.O. (No. 04780281).